Theory of unconfined excitons trapped by a quantum well

Guozhong Wen,* Peiji Zhao,† and Yia-chung Chang
Department of Physics and Material Research Laboratory, University of Illinois at Urbana-Champaign, 1110 West Green Street, Urbana, Illinois 61801
(Received 19 July 1996)

The energy levels and optical properties of unconfined excitons (excitons made of electron-hole pairs in the barrier material) interacting with a quantum well are studied via a variational method within the effective-mass approximation. The interplay of the relative motion and center-of-mass motion is examined carefully. The coupling of the unconfined excitons with the confined exciton via the emission of an acoustic phonon is examined. The effect of such coupling can produce much enhanced signals in the photoluminescence excitation (PLE) measurements. spectra. We perform simulation of the absorption and PLE spectra of an $In_xGa_{1-x}As/GaAs$ quantum well based on this mechanism and compare our results with the experiment performed by Reynolds *et al.* [Phys. Rev. B **43**, 1871 (1991)]. [S0163-1829(96)07547-9]

I. INTRODUCTION

In the last two decades a great deal of effort has been devoted to the study of confined excitons in quantum wells (QW) and superlattices.[1] Recently, Reynolds *et al.*[2] demonstrated the direct coupling of heavy-hole excitons in $In_xGa_{1-x}As/GaAs$ quantum wells with exciton states derived from the GaAs barrier. They observed that the photoemission due to heavy-hole exciton is enhanced substantially when the excitation energy is resonant with the GaAs-barrier exciton, indicating a direct coupling between the two. Although in Ref. 2, this exciton state is identified as the GaAs bulk exciton, we will show in this paper that it is more adequately described by an unconfined exciton trapped by the quantum well. Here and henceforth, we shall refer to the excitons derived from the barrier material of the quantum well system as the ''unconfined'' excitons in order to distinguish them from the confined excitons (i.e., excitons associated with confined subband states in the well). For confined excitons that are quasi-two-dimensional (2D), the electron and hole are confined to the well material so the center-of-mass (c.m.) motion along the z axis (growth axis) can be neglected; whereas for unconfined excitons (free or trapped), which are three dimensional (3D) in nature, the electron and hole are not confined to the well material, so their c.m. motion along the z-axis should be taken into account. Unlike the case of excitons in bulk, the Hamiltonian cannot be separated into the relative motion and the c.m. motion due to the presence of the quantum-well potential. Similar treatment can be used for excitons in very shallow quantum wells in which the confined and unconfined excitons can hardly be distinguished.[3,4]

Recent work by Griffiths *et al.*[5] revealed that the unconfined excitons may play a role in the photoluminescence spectrum. The interesting feature in their PL data is a peak (or a dip, depending on the pumping power) at the position just below the barrier bulk exciton energy. This feature is speculated as a barrier bulk exciton trapped by the quantum well. However, it remains unclear whether an unconfined exciton can become bound to the quantum well, and how large the binding energy can be. To study the interaction of the unconfined exciton with the quantum well we hereby perform a variational calculation to find the energy levels and wave functions for low-lying exciton states, taking into account the coupling of relative motion and the c.m. motion. The calculation is done with the use of two sets of trial wave functions. The first set (confined-exciton basis), which describes the confined exciton states, includes an ellipsoidal exciton wave function (with an anisotropy factor adjusted to model the transition from the 3D to 2D limit) multiplied by the subband envelope functions. The second set (c.m. motion basis), which describes the c.m. motion of the unconfined exciton states, includes a spherical 3D exciton wave function multiplied by Gaussian-like functions of the c.m. coordinate in the z direction.

We found that for a given well depth, there are multiple domains of the well width (W), within which a QW-trapped exciton state exists. To qualitatively describe such a trapped exciton state, we define a critical well width W_n, at which the energy of the nth confined exciton (obtained within the confined-exciton basis) coincides with the energy of a free barrier exciton. For $W<W_n$, the nth confined exciton is considered unbound within the confined-exciton basis. However, including the c.m.-motion basis lowers the energy of the state and the exciton becomes bound; thus, the mixed state is now more adequately described by a QW-trapped exciton. The trapping energy is usually smaller than the exciton binding energy. When the well width is further reduced to less than $W_n^0(<W_n)$, even including the c.m. motion basis will not produce a bound state. Thus (W_n^0, W_n) defines the domain in which the nth QW-trapped exciton exists. The significance of these QW-trapped excitons is that they can serve as a coupling medium in the photoluminescence excitation (PLE) measurements. This is because they have an extended length for the c.m. motion, thus a large oscillator strength, and at the same time they can couple strongly with the lowest confined exciton via a phonon emission process. We will show that it is the QW-trapped exciton that provides the much enhanced signal observed in the PLE spectrum reported by Reynolds *et al.*[2]

II. GENERAL THEORETICAL METHOD

We shall consider the $In_xGa_{1-x}As/GaAs$ strained quantum-well systems, in which the strain splitting of the heavy and light hole makes the valence-band mixing effect negligible. Neglecting valence-band mixing,[6] we can write the exciton Hamiltonian within the effective mass approximation as

$$H_{\rm ex}=-\nabla_1^2-\sigma_t\nabla_{\rho_2}^2-\sigma_l\nabla_{z_2}^2+V_1(z_1)+V_2(z_2)-\frac{2}{r_{12}},$$

where we have used the atomic units in which distance is measured in effective bohr, $a^*=\epsilon_0\hbar^2/m^e e^2$ and energy is measured in effective Rydberg, $R^*=e^2/2\epsilon_0 a^*$ (ϵ_0 is the static dielectric constant). $\sigma_t=m^e/m_t^h$ and $\sigma_l=m^e/m_l^h$ denote the ratio of electron effective mass (m^e) to the heavy-hole effective mass along the transverse (x,y) and longitudinal (z) directions. The subscripts 1 and 2 refer to the electron and hole, respectively. $V_1(z_1)$ and $V_2(z_2)$ are the quantum well potentials for the electron and hole.

To take into account the coupling of c.m. motion with internal motion the exciton trial wave function is expanded in terms of two sets of basis functions: Set one (confined-exciton basis) includes products of the confined exciton wave function $\phi_{cx}(r')$ and quantum-well subband envelope functions for the electron and hole, viz.,

$$\Psi_{nm}^{(1)}=\phi_{cx}(r')f_n(z_1)g_m(z_2),$$

where $\phi_{cx}(r')=e^{-\sqrt{x^2+y^2+\mu z^2}/a_x}$. a_x describes the exciton radius and μ describes the anisotropy of the exciton wave function. Both a_x and μ are treated as variational parameters. The envelope functions $f_n(z)[g_m(z)]$ are eigenfunctions of a single-particle Hamiltonian for an electron (hole) confined in a quantum-well potential:

$$H_{e(h)}=-\left(\frac{\partial}{\partial z}\right)^2+V_{e(h)}(z).$$

It has been shown that this set of trial functions describes the confined exciton states in quantum wells adequately.[7,8] Set two (c.m. motion basis) includes the products of a spherical barrier exciton wave function $[\phi_{bx}(r)]$ and Gaussian functions describing the center-of-mass motion, viz.,

$$\Psi_{\delta}^{(2)}=\phi_{bx}(r)e^{-\delta Z^2},$$

where Z is the center-of-mass coordinate in the z direction, and ϕ_{bx} is the barrier bulk exciton wave function, which takes the form of the ground-state wave function of hydrogen atom. Twenty different values of δ, which cover a large physically reasonable range, are used.

For ease in computing the Hamiltonian matrix elements, all envelope functions and exciton wave functions are written as linear combinations of a set of Gaussian functions. For example, f_n can be written as $f_n(z)=\Sigma_\beta C_n(\beta)e^{-\beta z^2}$ for even-parity states and $f_n(z)=\Sigma_\beta C_n(\beta)ze^{-\beta z^2}$ for odd-parity states. Then using a standard variational technique, we can solve this equation. The exponents β are chosen to be an ''even-tempered series,'' i.e., $\beta(i)=e_0e_p^{i-N_m}$, where $e_p=4.0$ a.u., $N_m=N_t/2+1$, N_t is the total number of parameters used, and e_0 is decided according to the width of the quantum well. In our calculations, we use $N_t=11$. The exciton wave function, $\phi_{cx}(r')$ is expanded in terms of four Gaussian-type orbitals with known coefficients,[9] viz.,

$$\phi_{cx}(r')=e^{-\sqrt{\rho^2+\mu z^2}/a_x}=\sum_{i=1}^{4}A_i a_x^{-3/4}e^{-\alpha_i/a_x^2(\rho^2+\mu z^2)},$$

with $\alpha_i=0.1233$, 0.4552, 2.0258, 13.7098 and $A_i=0.0756$, 0.1874, 0.1620, 0.0947 for $i=1$, 2, 3, 4. $\phi_{bx}(r)$ is just $\phi_{cx}(r)$ with a_x optimized for the barrier exciton.

To describe the hybridization of the unconfined excitons with the confined excitons, the total exciton wave function is expanded in the combined basis denoted ψ_N:

$$\psi_N=\Psi_{nm}^{(1)} \quad \text{for } N=1,\ldots,N_p,$$

$$\psi_N=\Psi_{\delta}^{(2)} \quad \text{for } N=N_p+1,\ldots,N_p+20,$$

where N_p is the total number of pairs of electron-hole product functions included in the calculation. We write

$$\Psi_{\rm ex}=\sum_N F(N)\psi_N.$$

Now the Schrödinger equation reads

$$H_{\rm ex}\Psi_{\rm ex}=E\Psi_{\rm ex}.$$

Projecting this equation on $\langle\psi_N|$ gives

$$\sum_{N'}\langle\psi_N|H|\psi_{N'}\rangle F(N')=E\sum_{N'}\langle\psi_N|\psi_N'\rangle F(N').$$

Note that our bases are nonorthogonal, i.e., $S(N,N')=\langle\psi_N|\psi_{N'}\rangle\neq\delta_{N,N'}$ in general, so we need to solve a generalized eigenvalue equation.

III. ABSORPTION COEFFICIENT AND PLE

After defining the confined-exciton basis (labeled I) and the c.m. motion basis (labeled Δ), we now expand the exciton wave function as

$$\Psi_{\rm ex}^i=\sum_I G(I)|I\rangle+\sum_\Delta G(\Delta)|\Delta\rangle$$

with $|I\rangle$ being the confined-exciton states:

$$|I\rangle=\sum_{nm}F(nm)|nm\rangle.$$

The oscillator strength for the ith exciton state is given by

$$f_i=C|\langle 0|\boldsymbol{\epsilon}\cdot\mathbf{p}|\Psi_{\rm ex}^i\rangle|^2$$
$$=CP_{cv}^2\left|\sum_I G(I)a_I+\sum_\Delta G(\Delta)a_c\right|^2,$$

where $P_{cv}=\langle U_c|\boldsymbol{\epsilon}\cdot\mathbf{p}|U_v\rangle$ is optical matrix elements between zone-center Bloch states (U_c and U_v) for the conduction and valence bands:

$$a_I=\phi_{cx}(0)\sum_{nm} F(nm)\int dz f_n(z)g_m^*(z),$$

$$a_c=\phi_{bx}(0)\frac{1}{\sqrt{A_\Delta}}\int dz e^{-\delta z^2}.$$

Note that in evaluating the above integrals, we have set $z_1=z_2=Z$ and $\rho=0$ (ρ is the radial coordinate for the in-plane relative motion).

The absorption coefficient is given by

$$\alpha(\hbar\omega)=C\sum_i f_i\delta(\hbar\omega-E_{\rm ex}^i).$$

The experiment that directly probes the properties of the unconfined exciton is the photoluminescence excitation measurement. In typical PLE measurements, one scans the incident photon energy from slightly above the lowest-lying exciton (LE) line to any desired higher energy, and measure the observed photoluminescence at the LE line as a function of the incident photon energy. When the excitation energy is high, the excited electron-hole pairs usually relax to the LE state via the multiphonon emission process, which is difficult to model accurately. Here, we consider a system in which the first excited state is an unconfined exciton state whose energy is close enough to the LE state such that the single-phonon emission process dominates. In this case, the PLE experiments probe the direct coupling strength of the unconfined exciton and the LE state mediated by an acoustic phonon.

The PLE spectrum for the case of direct coupling can be calculated by the perturbation theory similar to that for calculating the resonant Raman spectra (keeping only the most dominant terms), and we have

$$I(E)=|R_{fi}(E)|^2$$
$$=\sum_{q_z}\left|\sum_{\alpha,\beta}\frac{\langle 0|\hat{\boldsymbol\epsilon}_i\cdot\mathbf{p}|\alpha\rangle\langle\alpha|H_{\text{ex-ph}}|\beta;1_{\mathbf{q}}\rangle\langle\beta|\hat{\boldsymbol\epsilon}_s\cdot\mathbf{p}|0\rangle}{(E_i+i\Gamma-E_\alpha)(E_s+i\Gamma-E_\beta)}\right|^2$$
$$\times\delta(E_i-E_s+\hbar\omega_{\mathbf{q}}),$$

where $E(E_s)$ and $\hat{\boldsymbol\epsilon}_i(\hat{\boldsymbol\epsilon}_s)$ are the energy and polarization vector, respectively, of the incident (scattered) photon. $|0\rangle$ denotes the ground state of the solid, α and β label the possible excitonic excitations of the solid (intermediate states), $1_{\mathbf{q}}$ indicates a phonon of momentum $\mathbf{q}$ is created. Here we only consider the phonon-emission process, since the incident photon energy is always higher than the energy of the scattered photon. $H_{\text{ex-ph}}$ denotes the exciton-phonon interaction, and $\omega_{\mathbf{q}}$ denotes the phonon frequency associated with wave vector $\mathbf{q}\equiv(\mathbf{q}_\parallel,q_z)$. Γ is a phenomenological broadening parameter describing the finite lifetime of the intermediate states. Due to the conservation of in-plane momentum, $\mathbf{q}_\parallel$ must be equal to the difference of the in-plane wave vectors for the scattered and incident photons. The momentum conservation in the z direction is broken due to the presence of the quantum well; thus, we sum over all possible values of q_z in the above equation. Here, we are interested in shallow quantum wells, so the quantum confinement effect on phonons is small, so we can approximate the phonon modes by those of the host material.

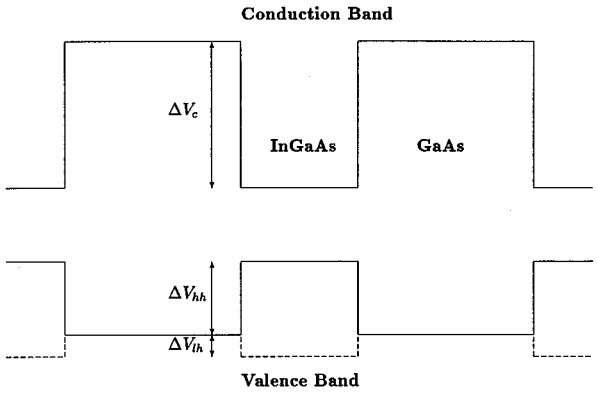

FIG. 1. Diagram for band edge lineup of $In_xGa_{1-x}As/GaAs$ quantum well.

For acoustic-phonon scattering, the exciton-phonon interaction is

$$H_{\text{ex-ph}}=iD_c\left(\frac{\hbar}{2MN\omega_{\mathbf{q}}}\right)^{1/2}\sum_{\mathbf{q}} q\{(a_{\mathbf{q}}^\dagger+a_{-\mathbf{q}})e^{i\mathbf{q}\cdot\mathbf{r}_1}$$
$$-b_a(a_{\mathbf{q}}^\dagger+a_{-\mathbf{q}})e^{i\mathbf{q}\cdot\mathbf{r}_2}\},\qquad(1)$$

with $b_a=D_v/D_c$, where $D_c(D_v)$ is the acoustic-phonon-deformation potential constant for the conduction (valence) band, M is the mass of the ion, N is the number of unit cells in the sample, $\omega_{\mathbf{q}}$ is the frequency of the acoustic phonon.

The matrix element for the exciton-phonon interaction can be written as

$$\langle\alpha|H_{\text{ex-ph}}|\beta\rangle=\gamma(\mathbf{q})I_{\alpha,\beta}(\mathbf{q}),$$

where $\gamma(\mathbf{q})=iD_cq(\hbar/2MN\omega_{\mathbf{q}})^{1/2}$. The integral $I_{\alpha,\beta}(\mathbf{q})$ is defined by

$$I_{\alpha,\beta}(\mathbf{q})=\int\Psi_\alpha^*(\mathbf{r}_1,\mathbf{r}_2)(e^{i\mathbf{q}\cdot\mathbf{r}_1}-b_ae^{i\mathbf{q}\cdot\mathbf{r}_2})\Psi_\beta(\mathbf{r}_1,\mathbf{r}_2)d\mathbf{r}_1d\mathbf{r}_2.\qquad(2)$$

IV. RESULTS AND DISCUSSION

We first consider $In_xGa_{1-x}As$-GaAs quantum wells with $x=0.1$. Due to lattice constant mismatch $In_xGa_{1-x}As$ layers experience substantial strain. The net effect of strain is to increase the band gap relative to the unstrained value and remove the degeneracy of the heavy- and light-hole bands at the Γ point. Following Ref. 10, we obtain the barrier heights for conduction and valence band:

$$\Delta V_c=76.8\ \text{meV},\quad \Delta V_{\text{hh}}=41.1\ \text{meV},\quad \Delta V_{\text{lh}}=-3.17\ \text{meV}.$$

This band edge lineup is shown in Fig. 1. For the electron and heavy hole, GaAs layers act as a barrier, while $In_xGa_{1-x}As$ layers act as a well. Since the light hole is expelled from the well region, the effect due to the light hole will be neglected in the present calculation. The parameters used in our calculation are listed in Table I.

TABLE I. Parameters used in current calculation.

	GaAs	InAs
m_c^* (m_0)	0.067	0.023
$m_{\rm hh}^*$ (m_0)	0.62	0.60
$m_{\rm lh}^*$ (m_0)	0.074	0.027
γ_1 (m_0^{-1})	7.65	19.67
γ_2 (m_0^{-1})	2.41	8.37
γ_3 (m_0^{-1})	3.28	9.29
E_g (meV)	1519	418
a (Å) lattice constant	5.6533	6.0584
ϵ_∞	12.35	14.6
a (eV) (defect potential)	-7.1	-5.9
b (eV) (defect potential)	-1.7	-1.8
C_{11} $(10^{11}$ dyn/cm$^2)$	11.88	8.33
C_{12} $(10^{11}$ dyn/cm$^2)$	5.38	4.53

Figure 2 shows low-lying energy levels of confined excitons (dashed lines) as functions of the well width W calculated by using the confined-exciton basis only (with optimized parameters a_x and μ). All energies are measured with respect to the GaAs (Γ point) band gap, which is taken as $E_G=1519$ meV. All exciton energies decrease with increasing well width since they basically follow the band-to-band transition energies. Here, we only include the basis functions in which either the conduction or heavy-hole subband is confined. For $W<50$ Å, only one conduction and one heavy-hole subband are confined. However, the exciton states derived from unconfined conduction (heavy-hole) subbands can become bound as long as they are paired up with one confined heavy-hole (conduction) subband. The physical origins of these exciton states are indicated in the figure. H1C1 denotes the lowest confined exciton derived from the first heavy-hole and conduction subbands. C1n denotes the exciton state derived from the first conduction and the nth heavy-hole subbands, while H1n denotes that derived from the first heavy-hole and nth conduction subbands. Note that only odd numbers of n are shown here, since the even number ones correspond to odd-parity states that are optically forbidden.

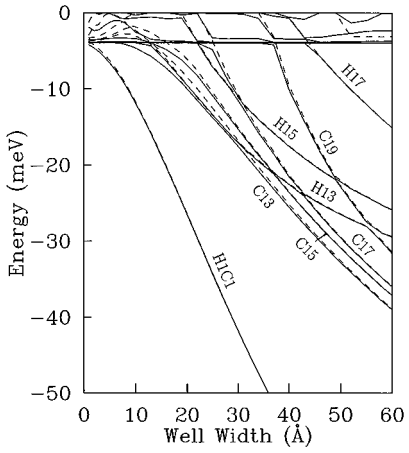

FIG. 2. Exciton energy levels of $In_{0.1}Ga_{0.9}As/GaAs$ quantum wells vs well width. Dashed lines: confined-exciton basis only. Solid lines: both confined-exciton and c.m. motion basis.

The exciton states derived from the second conduction (hole) subband and even-quantum number hole (conduction) subband would be optically allowed, but they are not bound for the well widths considered here, although the second heavy-hole subband is barely bound for $W>50$ Å. As expected, the energy of the lowest exciton level approaches the GaAs free exciton energy as the well width approaches zero.

The exciton energy levels calculated by including both the confined-exciton and c.m. motion bases versus well width (W) are also shown in Fig. 2 (solid curves). Additional states resulting from including the c.m.-motion basis are found to cluster around -3.93 meV, the ground-state energy of the GaAs bulk exciton. If infinite number of c.m. motion basis functions were used, we would expect a continuum spectra starting at -3.93 meV.

We note that the effect of the c.m. motion basis on the exciton states derived from the first heavy-hole subband (labeled H1n) is small, indicating that the confined-exciton basis with optimum parameters is adequate for getting the H1n series correctly. This means that the quantum-well trapped exciton state does not couple with the H1n series strongly. On the other hand, for the exciton states associated with the first conduction subband and higher heavy-hole subbands (C1n series), the inclusion of the unconfined exciton basis has an appreciable effect when the binding energy of the confined exciton is small. This is because the heavy-hole mass is much larger than the electron effective mass, so the c.m. motion wave function for the quantum-well trapped exciton resembles the heavy-hole envelope function and it couples strongly with C1n excitons.

We can now qualitatively describe the trapping of a barrier exciton by the $In_xGa_{1-x}As$ QW as follows. When the well width W increases from zero, the barrier exciton, which is trapped by the quantum well, immediately turns into the confined H1C1 exciton, since for any finite width there exists a confined state (for both the electron and hole). When W further increases to around 8 Å, another exciton state becomes trapped. Since the total wave function must remain orthogonal to the lower-lying exciton state (in this case, H1C1) and the c.m. motion resembles the heavy-hole envelope function, this state gradually turns into the C13 exciton state as W goes beyond 15 Å. (Recall that here we only consider the exciton states with overall even parity. If odd-parity states are also of interest, there will be another quantum-well trapped exciton occurring at smaller W and it will turn into the C12 exciton.) The next QW-trapped exciton (QWTE) occurs at around $W=14$ Å and turns into the C15 exciton at $W\approx18$ Å. We define the trapping energy as the difference in energy between the dashed and solid curves. The strongest trapping occurs at the onset where the confined exciton becomes bound. For this case, the maximum trapping energies are approximately 2, 1, and 0.9 meV for the C13, C15, and C17 excitons, respectively.

Next we consider $In_xGa_{1-x}As$-GaAs quantum wells with the well width fixed at 17 Å (corresponding to 6 ML), but with different In mole fraction x. The low-lying energy levels of excitons obtained with and without the c.m. motion basis as functions of the In mole fraction (x) are shown in Fig. 3. Again, the trapping of unconfined excitons occurs when the well depth is barely deep enough to bind an exciton

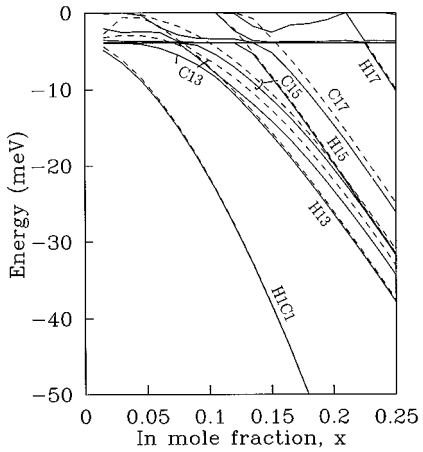

FIG. 3. Exciton energy levels of $In_xGa_{1-x}As/GaAs$ quantum wells vs the In mole fraction (x). Dashed lines: confined-exciton basis only. Solid lines: both confined-exciton and c.m. motion basis.

associated with the first conduction subband and a higher-lying heavy-hole subband The maximum trapping energies are around 1–2 meV.

Figure 4 shows the calculated absorption and PLE spectra of a $In_xGa_{1-x}As$-GaAs quantum well with $W=17$ Å and $x=0.05$. We choose this quantum well in order to compare our results with the experiment performed by Reynolds *et al.*[2] In Ref. 2, the intended In mole fraction was $x=0.1$. However, we found that in order to match the observed H1C1 exciton energy, we have to use $x=0.05$. If we use $x=0.1$, the H11 exciton energy would be 20 meV below the GaAs band gap (see Fig. 3). This discrepancy could be due to the uncertainty in the x value in the experiment or the valence-band offsets assumed here. A constant band gap was added to all exciton levels, so the location of the free GaAs exciton (at 1.515 eV) matches the experiment. Since the total oscillator strength of the barrier exciton depends on the sample size and the penetration depth of the incident photon (both are of the order of 10 000 Å), we therefore add a confining potential, which has a height of 10 eV (for both electrons and holes) and width of 10 000 Å to the single-quantum-well system considered here. The center of the confining potential well and that of the single quantum well are assumed to coincide. The absorption spectrum (dashed curve) displays three peak structures corresponding to the H1C1 exciton, the QW-trapped exciton, and the free barrier exciton, respectively. Since we used a variational method, the continuum states are not modeled properly, so the absorption due to the continuum states is missing. We found that the oscillator strength of the QW-trapped exciton (peak structure at 1.5147 eV) is stronger than the H1C1 exciton (by about a factor 1.5). According to Rashba's theory,[11] the oscillator strength of a trapped exciton is proportional to the volume covered by the c.m. motion of the exciton. This indicates that the volume covered by the c.m. motion for the QW-trapped exciton is at least 1.5 times that of the H1C1 exciton for this quantum well. Note that if the c.m. motion part is ignored, the QW-trapped exciton would turn into the confined C13 exciton, which should have almost zero oscillator strength due to the $\Delta n=0$ selection rule normally applied to confined excitons in quantum wells.[12] The fact that we get larger oscillator strength than the H1C1 exciton here indicates that the state is more adequately described by a QW-trapped exciton than just a modified C13 confined exciton.

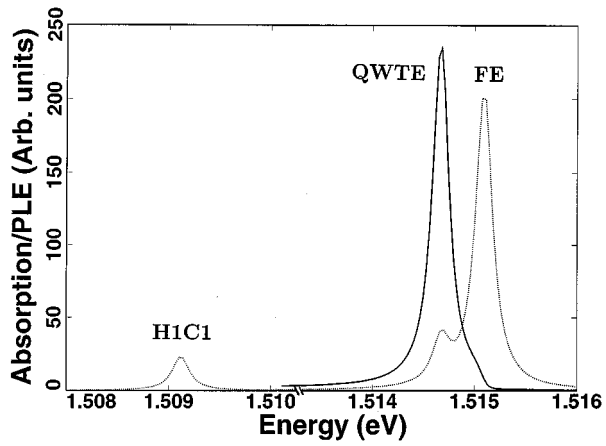

FIG. 4. Calculated absorption (dashed) and PLE (solid) spectra of a $In_{0.05}Ga_{0.95}As/GaAs$ quantum well with $W=17$ Å. The broadening parameter (Γ) used is 0.1 meV.

The oscillator strength of the free GaAs exciton is even larger, since the volume covered by it is larger. In fact, if we did not restrict the range in the z direction for the GaAs free exciton due the finite sample size, its theoretical strength would have been infinite.

In the PLE spectrum (solid curve), the strength of the QWTE becomes much larger than that of the free GaAs exciton (which appears as a weak shoulder structure at 1.5151 eV). This is because the electron-phonon coupling strength favors the QW-trapped exciton much more. According to Eq. (4), the coupling matrix element due to emission of an acoustical phonon is proportional to the wave vector q (or q_z, since $q_\parallel=0$ for the case considered here), which is inversely proportional to the range covered by the wave function (L) in the z direction. Thus the coupling strength is inversely proportional to L^2, which outweighs the oscillator strength factor. Furthermore, the coupling matrix is also proportional to the overlap integral given in Eq. (2), which again favors the QW-trapped exciton, since it is more localized at the quantum well.

We now compare our PLE spectrum with that observed by Reynolds *et al.* (see Fig. 2 of Ref. 2). We noted that in Ref. 2 a strong peak and a shoulder structure were observed at 1.5147 and 1.5152, respectively. We believe that the strong peak is due to the QW-trapped exciton, while the shoulder structure is due to the free GaAs exciton. The shoulder structure observed in Ref. 2 is stronger than the one calculated theoretically. This may due to the higher-order phonon emission process, which is ignored here. When the first-order coupling is weak as for the FE case, the higher-order process may become important. The spacing between the two structures is about 0.5 meV, while our calculated spacing is about 0.41 meV. The discrepancy may be attributed to the interface roughness in the sample, the uncertainty in the well width and barrier height, and the fact that we have ignored the valence-band mixing effect[6] in the calculation.

V. SUMMARY

In conclusion, we have studied the 3D bulk excitons trapped by a quantum well and coupled with the confined excitons. The trapping occurs when the higher-lying confined excitons are nearly unbound, and the interaction of unconfined and confined exciton states is strong. The trapping energy is less than the binding energy of a free exciton with a maximum around 2 meV for the case considered here. We found that the QW-trapped exciton state plays an important role in the PLE spectrum for very narrow or shallow quantum wells because it enhances the signal via direct coupling with the lowest-lying exciton state. Our calculated PLE spectrum for a $In_xGa_{1-x}As$-GaAs quantum well is in fair agreement with that observed by Reynolds *et al.*[2]

ACKNOWLEDGMENTS

We would like to thank C. O. Griffiths and M. V. Klein for fruitful discussions. This work was supported by the Office of Naval Research (ONR) under Contract No. N00014-90-J-1267 and the University of Illinois Materials Research Laboratory through Contract No. NSF/DMR-89-20538.

*Current address: Department of Physics, University of Houston, Houston, Texas.

†Current address: Department of Physics, Stevens Institute of Technology, Hoboken, New Jersey.

[1] See, for example, G. D. Sanders and K. K. Bajaj, Phys. Rev. B **35**, 2308 (1987).

[2] D. C. Reynolds, K. R. Evans, K. K. Bajaj, B. Jogai, C. E. Stutz, and P. W. Yu, Phys. Rev. B **43**, 1871 (1991).

[3] I. Brener, W. H. Knox, K. W. Goossen, and J. E. Cunningham, Phys. Rev. Lett. **70**, 319 (1993).

[4] J. Warnock, B. T. Jonker, A. Petrou, W. C. Chou, and X. Liu, Phys. Rev. B **48**, 17 321 (1993).

[5] C. O. Griffiths, D. R. Wake, M. V. Klein, J. J. Alwan, and J. J. Coleman, Bull. Am. Phys. Soc. **37**, 688 (1992)

[6] See, for example, Y. C. Chang and J. N. Schulman, Appl. Phys. Lett. **43**, 536 (1983); Phys. Rev. B **31**, 2069 (1985).

[7] R. L. Greene and K. K. Bajaj, Solid State Commun. **45**, 831 (1983).

[8] G. D. Sanders and Y. C. Chang, Phys. Rev. B **32**, 5517 (1985).

[9] C. M. Reeves, J. Chem. Phys. **39**, 1 (1963).

[10] Geoffrey Duggan, Karen J. Moore, Karl Woodbridge, Christine Roberts, Nicolas J. Pulsford, and Robin J. Nicholas (unpublished).

[11] E. I. Rashba and G. E. Gurgenishvili, Fiz. Tverd. Tela (Leningrad) **4**, 1029 (1962) [Sov. Phys. Solid State **4**, 759 (1962)].

[12] R. Dingle, *Festkorperprobleme*, edited by J. Trensch (Pergamon, New York, 1975), Vol. 15, p. 21.